

• **Technical note**

## New approach for attenuation correction in SPECT images, using linear optimization

**A. Vahidian Kamyad<sup>1</sup>, M.H. Noori Eskandari<sup>1</sup>, M. Naji Midani<sup>2</sup>,  
M. Hajizadeh Saffar<sup>2\*</sup>**

<sup>1</sup>Department of Mathematic, Ferdowsi University, Mashad, Iran

<sup>2</sup>Department of Medical Physics, Mashad University for Medical Sciences, Mashad, Iran

**Background:** Photon attenuation as an inevitable physical phenomenon influences on the diagnostic information of SPECT images and results to errors in accuracy of quantitative measurements. This can be corrected via different physical or mathematical approaches. As the correction equation in mathematical approaches is nonlinear, in this study a new method of linearization called 'Piece Wise Linearization' (PWL) is introduced and to substantiate its validity for SPECT image reconstructions, a phantom study is performed. **Material and Methods:** A SPECT scan of a homemade heart phantom filled with 2 mCi <sup>99m</sup>Tc was acquired by dual head Siemens E.Cam gamma camera equipped with LEHR collimator. Row data of the scan were transferred in DICOM format to a pc computer for reconstruction of the images using MLEM iterative algorithm in Matlab software. **Result:** Attenuation map of the phantom  $\mu(x)$  were derived using PWL with linear optimization approach. Based on that, the attenuation corrected SPECT image of the phantom were reconstructed and compared with non-corrected image, using MLEM iterative algorithm. Comparison of the corrected and non-corrected images confirmed with CT attenuation correction method. **Conclusion:** Attenuation correction in SPECT image can be achieved successfully, using emission data and piecewise linearization with linear optimization approach. The corrected image of  $f(x)$  and attenuation map  $\mu(x)$  of the heart phantom using this approach promise acceptable image quality for diagnostic clinical use. **Iran. J. Radiat. Res., 2010; 8 (2): 111-116**

**Keywords:** Piece wise linearization, linear optimization, SPECT image, attenuation correction.

### INTRODUCTION

Photon attenuation is an inevitable physical phenomenon that influences diagnostic information of SPECT images

and results to errors in Accuracy of quantitative measurements. This effect is especially significant in regions of body that have inhomogeneous distribution of attenuation coefficient such as lungs and heart <sup>(1)</sup> e.g. attenuation of breast in women results to erroneous diagnosis of heart defect.

Study of scatter or attenuation correction in SPECT images is generally performed to discuss methods used to estimate the unknown tissues attenuation map  $\mu(x)$  via physical approach of extra transmission scans (simultaneously or in succession with emission scan) <sup>(2)</sup> or mathematically approach through modification of emission data or using those to estimate the attenuation map. History and several analytical attenuation correction methods have been reviewed by Gourion D *et al.* 2002, and they described a method based on nonlinear optimization program for estimation of attenuation map using SPECT emission data <sup>(3)</sup>. As the linear optimization programs (LOP) are more power full and easy to use than the nonlinear, this study is planned to simplify the method by using LOP. In this method the nonlinear equations will convert to linear ones, using new piece wise linearization (PWL) method, and substantiate its validity using a phantom

#### \*Corresponding author:

Dr. M. Hajizadeh Saffar,  
Department of Medical Physics, Mashad University for  
Medical Sciences, Mashad, Iran.

Fax: +98 511 8002320

E-mail: [hajizadeh@mums.ac.ir](mailto:hajizadeh@mums.ac.ir)

study.

## MATERIALS AND METHODS

### Formulation of the problem

Let  $f(x)$  and  $\mu(x)$  denote the emission source of radionuclide distribution and attenuation coefficient of point  $x$  of the body tissue. The intensity of radiation emitted in different directions perpendicular to the surface of Gamma camera can be measured as projections. In SPECT technique, images of the radionuclide distribution  $f(x)$  and attenuation coefficient of the body tissue  $\mu(x)$  can be simultaneously estimated from measured projections, using attenuated radon transform by the following formula <sup>(3)</sup>:

$$R_{[\mu]}f(s, \theta) \equiv \int_{-\infty}^{+\infty} f(s\theta + t\theta^\perp) e^{-\int_t^\infty \mu(s\theta + t\theta^\perp) d\tau} dt = g(s, \theta)$$

Here  $g(s, \theta)$  is the datum acquired on the line referenced by  $(s, \theta)$ . Radon transform can be solved using numerical techniques <sup>(4)</sup>. The attenuated radon transform in the discrete form is shown as follow:

$$R_{[\mu]}f \equiv \sum_j f_j a_{i,j} e^{-\sum_{k \in k_{i,j}} r_{i,k} \mu_k} = g_i \quad i = 1, 2, \dots, n$$

Where  $j$  is the number of image pixels in a defined slice of the subject and  $i$  the identification number of detectors around of that.  $f_j$  is the pixel value of the image, proportional to the number of radionuclide disintegration in voxel  $j$ ,  $g_i$  the sinogram measured data from  $i$ th detection bin in gamma camera,  $a_{i,j}$  the elements of the system matrix or detection probability of emitted photons from voxel  $j$  of the subject to be detected in  $i$ th detection bin in gamma camera and is dependent to physical radiation model, collimator specification and radiation detection geometry of gamma camera <sup>(5)</sup>,  $r_{i,k}$  and  $\mu_k$  are respectively the length and attenuation coefficient of pixel  $k$  which is along the direction of pixel  $j$  to

detection bin  $i$ . As the disintegration of radionuclide and their detections are two Poisson independent variables, therefore,  $g_i$  is a Poisson variable and its mathematical expectancy is  $E(g_i) = \sum_{j=1}^m f_j a_{i,j} = (Af)_i$ . From this equation the  $f_j$  can be estimated using likelihood maximization equation  $L(f)$ . To maximize  $L(f)$ , we usually maximize  $\text{Log}(L(f))$ , therefore, estimation of  $f_j$  for an image with  $m$  pixel of soft tissue ( $\mu = 0.15 \text{ pixel}^{-1}$ ) to be reconstructed from  $n$  measured data bin, can be achieved from derivative of the  $\text{Log}(L(f))$ , or using optimization model such as follow <sup>(3)</sup>:

$$\min_{f, \mu} \sum_{i=1}^n \sum_{j=1}^m [f_j a_{i,j} - q_{i,j} \log(f_j a_{i,j})]$$

Such that  $0 \leq \mu_j \leq .15$  and  $f_j \geq 0$

$$j = 1, 2, \dots, m \quad (1)$$

Where  $a_{ij} \equiv a_{ij}(\mu)$  and  $a_{ij}(\mu) = a_{ij} e^{-\sum_{k \in k_{i,j}} r_{i,k} \mu_k}$  and  $q_{ij} = g_i \frac{a_{ij}(\mu) f_j}{\sum_{k=1}^m a_{ik}(\mu) f_k}$  which is consistence with  $g_i = \sum_{j=1}^m q_{ij}$ . To avoid cross talk between simultaneously estimation of the unknown attenuation map  $\mu_j$  and emission source  $f_j$  from emission measured data  $g_i$ , and matching the data with acceptable error tolerance some investigators used an appropriate regularization term,  $al[\mu, f]$  or other possible choices of regulators adapted to the problem <sup>(3, 6, 7)</sup>,

As application of linear optimization is much easier than nonlinear, especially for too many unknown parameter from two variables  $\mu_j, f_j$  ( $j = 1, 2, 3, \dots, m$ ) and such power of nonlinearity of the objective function, we decide firstly to simplify the objective function and then convert it to a linear one, using PWL method. To simplify the objective function we assumed  $\sigma_j(\mu) = \sum_{i=1}^n a_{ij}(\mu)$  as a function of  $\mu$  and  $\tau_j^{(k)} = \sum_{i=1}^n q_{ij}^{(k)}$  for step  $k$  in the iteration process. Replacing those in problem 1 will simplify it

as follow:

$$\min_{f, \mu} \sum_{j=1}^m [f_j \sigma_j(\mu) - \tau_j^{(k)} \log f_j] - \sum_{i=1}^n \sum_{j=1}^m q_{ij}^{(k)} \log(a_{ij}(\mu)) \quad (2)$$

Assuming there is a known  $\mu^{k+1}$  in step  $k + 1$ , the unknown  $f^{k+1}$  can be calculated from  $f^{k+1} = \frac{\tau^k}{\sigma(\mu^{k+1})}$ , using MLEM formula. Substituting that in problem 2, will omit  $f_j$  from optimization problem 2 and  $\mu^{k+1}$  can be estimated for next iteration step from the following problem:

$$\min_{\mu} \sum_{j=1}^m \tau_j^k \log \sigma_j(\mu) - \sum_{i=1}^n \sum_{j=1}^m q_{ij}^k \log(a_{ij}(\mu))$$

Such that  $0 \leq \mu_j \leq 0.15, j = 1, 2, \dots, m$  (3)

This is more simplified than problem 2, but still nonlinear and to linearize that, one should first expand the  $\log a_{ij}(\mu)$ , using  $\log x e^{-y} = -y + \log x$ , and eliminate  $\sum_{i=1}^n \sum_{j=1}^m q_{ij}^k \log(a_{ij})$  which is constant and has no effect on optimization, and then linearize the  $\log \sigma_j(\mu)$  using PWL method. Thus problem 3 convert to following problem:

$$\min_{\mu} \sum_{j=1}^m \tau_j^{(k)} \log \sigma_j(\mu) + \sum_{i=1}^n \sum_{j=1}^m q_{ij}^k \sum_{k \in K_{ij}} r_{ik} \mu_k$$

Such that  $0 \leq \mu_j \leq 0.15, j = 1, 2, \dots, m$  (4)

Linearization of the  $\log \sigma_j(\mu)$  using PWL method can be achieved by using first order Taylor expansions, first for  $e^{-\sum_{k \in K_{ij}} r_{ik} \mu_k}$  and then for the  $\log$  term. As this approach is not a precise method and has a large error, it should be performed on small sub intervals of the variables to get a feasible estimation of  $\mu(x)$  and reduce the error. Mathematical proof and validity of this approach has been reported by (8).

$$\sum_{j=1}^m \tau_j \log \sigma_j(\mu) + \sum_{i=1}^n \sum_{j=1}^m q_{ij} \sum_{k \in K_{ij}} r_{ik} \mu_k \cong \sum_{j=1}^m \tau_j \left( \text{const}(j, p, q) - \sum_{i=1}^n a_{ij} e^{-s_p} \frac{1}{w_q} \sum_k r_{ik} \mu_k \right) + \sum_{i=1}^n \sum_{j=1}^m q_{ij}^k \sum_{k \in K_{ij}} r_{ik} \mu_k$$

As  $e^{-\sum_{k \in K_{ij}} r_{ik} \mu_k}$  for  $i = 1, 2, \dots, n$  &  $j = 1, 2, \dots, m$  are in the domain of,  $a \leq \sum_{k \in K_{ij}} r_{ik} \mu_k \leq b$ , and  $[a, b]$  interval can be divided into  $l_1$  equally subintervals such that  $a = y_1 < y_2 < \dots < y_{l_1} = b$  and a midpoint in the  $p$ th subinterval,  $A_p = [y_p, y_{p+1}]$  denote  $s_p = \frac{y_p + y_{p+1}}{2}$  for  $p = 1, 2, \dots, l_1$ , the first order Taylor expansion of  $e^{-x}$  in the subinterval  $[y_p, y_{p+1}]$  around  $s_p$  is estimated as  $e^{-x} \cong e^{-s_p} + (x - s_p)(-e^{-s_p})$  which would be as follow for  $x = \sum_{k \in K_{ij}} r_{ik} \mu_k \in A_p$ :

$$e^{-\sum_{k \in K_{ij}} r_{ik} \mu_k} \cong e^{-s_p} + \left( \sum_{k \in K_{ij}} r_{ik} \mu_k - s_p \right) (-e^{-s_p})$$

This approach has an error of the order  $O((x - s_p)^2)$  (9) and would decrease using more points in  $[a, b]$  by selecting smaller subintervals. The same approach can be used for  $c \leq \sum_{i=1}^n a_{ij} e^{-\sum_{k \in K_{ij}} r_{ik} \mu_k} \leq d$ , dividing  $[c, d]$  to  $l_2$  equally subintervals such that  $c = z_1 < z_2 < \dots < z_{l_2} = d$  and a midpoint  $w_q = \frac{z_q + z_{q+1}}{2}$  in the  $q$ th subinterval  $B_q = [z_q, z_{q+1}]$  for  $q = 1, 2, \dots, l_2$ . First order Taylor expansion of  $\log z$  around  $w_q$  in the subinterval  $[z_q, z_{q+1}]$  for  $z_q \leq z = \sum_{i=1}^n a_{ij} e^{-\sum_{k \in K_{ij}} r_{ik} \mu_k} \leq z_{q+1}$  is as follow with an error of the order  $O((x - w_q)^2)$ .

$$\log \sigma_j(\mu) = \log \left( \sum_{i=1}^n a_{ij} e^{-\sum_k r_{ik} \mu_k} \right) = \log(w_q) + \left\{ \sum_{i=1}^n a_{ij} e^{-\sum_k r_{ik} \mu_k} - w_q \right\} \left( \frac{1}{w_q} \right)$$

Substituting the constant value  $\text{const}(j, p, q) = \log(w_q) + \sum_{i=1}^n a_{ij} e^{-s_p} \frac{1}{w_q} (s_p + 1) - 1$  for each  $j, p$  &  $q$  over subinterval of  $A_p$  and  $B_q$ , would summarize the optimization problem 4 as follow:

$$\cong \text{const}(p, q) + \sum_{i=1}^n \sum_{j=1}^m \left( q_{ij} - \tau_j a_{ij} e^{-s_p} \frac{1}{w_q} \right) \sum_{k \in k_{ij}} r_{ik} \mu_k = \text{const}(p, q) + \sum_{l=1}^m C_l^{p,q} \mu_l$$

For more simplification we used  $\text{const}(p, q) = \sum_{j=1}^m \tau_j \text{const}(j, p, q)$ , and the rest as  $\sum_{l=1}^m C_l^{p,q} \mu_l$ . Thus we have a linear optimization problem for estimating attenuation map,  $\mu(x)$ , which can use *linprog* function in Matlab software. Constrains to be used in the optimization problem can be derived from  $[a, b]$  and  $[c, d]$  intervals' boundary. As we assumed  $\sum_{k \in k_{ij}} r_{ik} \mu_k \in [y_p, y_{p+1}]$  and  $\sum_{i=1}^n a_{ij} e^{-\sum_{k \in k_{ij}} r_{ik} \mu_k} \in [z_q, z_{q+1}]$  for any  $i$  &  $j$ , therefore,  $y_p \leq \sum_{k \in k_{ij}} r_{ik} \mu_k \leq y_{p+1}$  and  $m e^{-y_{p+1}} \leq \sum_{i=1}^n a_{ij} e^{-\sum_{k \in k_{ij}} r_{ik} \mu_k} \leq M e^{-y_p}$  assuming  $M = \max \sum_{i=1}^n a_{ij}$  and  $m = \min \sum_{i=1}^n a_{ij}$ , which means, for any  $p$  the valid indices of  $q$  should fulfill the non-equalities of  $m e^{-y_{p+1}} \leq z_q \leq \sum_{i=1}^n a_{ij} e^{-\sum_{k \in k_{ij}} r_{ik} \mu_k} \leq z_{q+1} \leq M e^{-y_p}$ .

Also, using first order Tayloer expansion of  $\sum_{i=1}^n a_{ij} e^{-\sum_{k \in k_{ij}} r_{ik} \mu_k}$  at  $s_p$  midpoint of  $[y_p, y_{p+1}]$  for  $p = 1, 2, \dots, l_1$  and  $q = 1, 2, \dots, l_2$ , assuming  $\text{con}(j, q) = \sum_{i=1}^n a_{ij} e^{-s_p}$  would result:

$$\sum_{i=1}^n a_{ij} e^{-\sum_{k \in k_{ij}} r_{ik} \mu_k} \cong \text{con}(j, q) - \sum_{i=1}^n a_{ij} e^{-s_p} \sum_{k \in k_{ij}} r_{ik} \mu_k$$

That means the optimization should fulfill the following constrains:

$$\begin{aligned} -z_{q+1} + \text{con}(j, q) &\leq \sum_{i=1}^n a_{ij} e^{-s_p} \sum_{k \in k_{ij}} r_{ik} \mu_k \\ &\leq -z_q + \text{con}(j, q) \\ &j = 1, 2, \dots, m \end{aligned}$$

Therefore the aim of the study substantiate, by finding  $\mu$  vector so that minimize the linear function of  $\text{const}(p, q) + \sum_{l=1}^m C_l^{p,q} \mu_l$  with respect to  $\mu$ . This can be achieved by assuming optimal solution  $[\mu^{p,q}, \min^{p,q}]$ , as the optimization of:

$$\min_{\mu} \sum_{l=1}^m C_l^{p,q} \mu_l \quad (5)$$

$$\begin{aligned} \text{such that } y_p &\leq \sum_{k \in k_{ij}} r_{ik} \mu_k \leq y_{p+1} \\ i &= 1, 2, \dots, n \text{ \& } j \in D_i \\ z_{q+1} + \text{const}(j, q) &\leq \sum_{i=1}^n a_{ij} e^{-s_p} \sum_{k \in k_{ij}} r_{ik} \mu_k \\ &\leq -z_q + \text{const}(j, q) \\ &j = 1, 2, \dots, m \\ 0 &\leq \mu_j \leq 0.15 \quad j = 1, 2, \dots, m \end{aligned}$$

Where  $D_i$  consists of image pixels which are along the direction of pixel  $j$  to detection bin  $i$ . Assuming  $\min^{p^*, q^*} = \min_{p, q \in E_p} (\min^{p, q} + \text{const}(p, q))$  denote the  $\mu$  vector which is  $\mu^{k+1} = \mu^{p^*, q^*}$ , the attenuation map  $\mu(x)$  for next iteration, this leads to attenuation corrected emission image of  $f(x)$  from  $f_j^{k+1} = \tau_j^k / \sigma_j(\mu^{k+1})$ .

### Measurements set up

To substantiate this method in reconstruction and attenuation correction of SPECT heart images, a heart and chest phantom which consists of 4 cylinders, as shown in figure 1, were made and filled with water to represent the soft tissue, except in spaces for lungs, and 2mCi of  $^{99m}\text{Tc}$  pertechnetate is added in the heart wall and body contour. A SPECT of the phantom were acquired, using 32 projections of  $64 \times 64$  pixels in arc of 180 degree, by Siemens dual head E.Cam gamma camera with LEHR collimator. Time of each projection was 25 seconds, similar to myocardial perfusion SPECT in patients. Row data of the SPECT were transferred in DICOM format to a pc computer as a three dimension matrix with  $64 \times 64 \times 32$  elements for reconstruction of the images with a written program <sup>(10)</sup>, using MLEM algorithm in Matlab software.



**Figure 1.** Transverse section of the heart and chest phantom composed of four cylinders, 15 cm long, which represent soft tissue of body contour, lungs, heart wall, and internal blood of the heart.

In this program a non-corrected tomogram of the predefined slice of the phantom was calculated  $f^0$ , using first iteration of MLEM algorithm and zero attenuation map  $\mu^0 = 0$ ,<sup>(8)</sup>. Base on this image data and its sinogram  $g_i$ , values of  $q_{i,j}$  and  $\tau_j$  were calculated to be used with system matrix  $a_{i,j}$  for estimation of attenuation map for next iteration  $\mu^{k+1}$  through optimization of  $\sum_{l=1}^m C_l^{p,q} \mu_l = \sum_{i=1}^n \sum_{j=1}^m \left( q_{ij} - \tau_j a_{ij} e^{-s_p \frac{1}{w_q}} \right) \sum_{k \in k_{ij}} r_{ik} \mu_k$  with constrains used in problem 5. The attenuation corrected emission SPECT image of the next iteration can then be calculated from  $f_j^{k+1} = \tau_j^k / \sigma_j(\mu^{k+1})$ .

## RESULTS AND DISCUSSION

A sinogram of a predefined slice were first selected as a matrix with  $64 \times 32$  elements and SPECT image of that were reconstructed using MLEM iterative algorithm with no attenuation correction. The image is shown in figure 2.

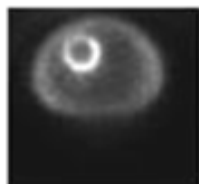


**Figure 2.** A  $64 \times 64$  pixels SPECT image of the heart and chest phantom reconstructed by 5 iteration of MLEM algorithm with no attenuation correction.

To derive attenuation map  $\mu(x)$  using PWL with linear optimization approach, as described in problem 5, the *linprog* code of Matlab software has been used. The numbers of variables in each image,  $m=64 \times 64=4096$ , and constrains in problem 5 which are  $\#m^2$ , exceeds the capacity of *linprog* code in Matlab software. to overcome this problem and also to reduce the time of calculations, it was decided firstly, to reduce the size of the attenuation map to  $32 \times 32$  pixels, and then decrease the number of constrains in optimization process, using only one constrain in a detection bin. These simplifications can lead to estimate a poor resolution attenuation map as shown in figure 3a. As the resolution of the attenuation map  $\mu(x)$ , actually need not to be as fine as that of the emission image  $f(x)$ <sup>(3)</sup>, it was then used to derive the attenuated corrected image of the phantom. The emission SPECT image of a heart phantom with attenuation correction was reconstructed and shown in figure 3b, to be compared with non-corrected image of figure 2.

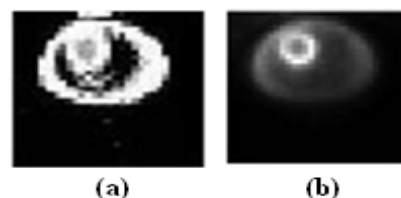


**Figure 3.** Attenuated corrected emission image  $f(x)$  and attenuation map  $\mu(x)$  of the heart and chest phantom reconstructed by PWL method.

The ratio of the activity of the deeper points (heart wall) to the surfaces (body contour) in the attenuated corrected image of figure 3b has increased with respect to non-corrected ones in figure 2. This is confirmed with the results of CT attenuation correction method<sup>(11)</sup>, and means that the attenuation correction has been achieved successfully by the PWL mathematical approach.



## CONCLUSION

The attenuated corrected emission image  $f(x)$  and attenuation map  $\mu(x)$  of the phantom using one iteration and simplified optimization process matches well with non-corrected image in figure 2, except on some pixels adjacent the tissue walls. Contrast of the body contour in the corrected emission image is lower than that in figure 2, which is due to attenuation correction procedure, leading to higher radionuclide emission of the heart wall. The results indicate attenuation correction has been achieved successfully by the PWL mathematical approach, and of course using faster computer and more iteration would presumably improve the results and can performed images with higher resolution in appropriate time. Therefore, it is concluded that attenuation correction using emission data only can be performed in SPECT images with PWL and linear optimization approach and provide acceptable image quality for diagnostic clinical use.

## ACKNOWLEDGMENT

Cooperation of computer centers in medical school of Mashad University of Medical Science and mathematical faculty of Ferdowsi University is fully appreciated.

## REFERENCES

1. Zaidi H (2006) *Quantitative analysis in nuclear medicine imaging*. New York: Springer Science Business Media, Inc
2. Celler A, Axen D, Togane D, El-khatib j (2000) *Investigation of scatter in SPECT transmission studies*. IEEE Trans. Nucl Sci, **47**: 1251-1256.
3. Gorion D, Noll D, Gantet P, Celler A, Esquerre JP (2002) *Attenuation correction using SPECT emission data only*. IEEE Trans. Nucl Sci, **49**: p. 2172-2179.
4. Bronnikov AV (1999) *Numerical solution of the identification problem for the attenuated radon transform*. Inverse Problems, **15**: 1315-1324.
5. Hajizadeh M, Zakavi SR, Momen-Nejad M, Naji M (2008) *Evaluation the role of system matrix in SPECT images reconstructed by OSEM technique*. Iran J Nucl Med, **16**: 31-36.
6. Dicken V (1998) *Simultaneous activity and attenuation reconstruction in single photon emission computed tomography, a nonlinear illposed problem*. PhD Thesis, Potsdam University, Potsdam/Germany.
7. Dicken V (1999) *Simultaneous activity and attenuation reconstruction in emission tomography*. Inverse Problems, **15**: 931-960.
8. Noori Eskandari MH (2008) *Determination of attenuation map and corrected images in SPECT by mathematics programming*, MSc thesis in Mathematics Dept. Ferdosi University, Mashad/Iran.
9. Atkinson, K.E. An introduction to numerical analysis, second edition, John Wiley & sons, Inc.1989
10. Naji M (2007) *Evaluation of attenuation correction methods in heart SPECT images and optimization of chosen method using phantom*, MSc thesis in Medical physics Dept. Mashad university of medical science, Mashad/Iran.
11. Naji M, Zakavi SR, Hajizadeh M, Momennezhad M (2008) *Evaluation of Attenuation Correction Process in Cardiac SPECT Images*. Iran J Nucl Med, **16**: 1-7.